TOWARDS AN EXTENSION OF TFC MODEL OF PREMIXED TURBULENT COMBUSTION

V. Sabel'nikov* and A. Lipatnikov**
e-mail: Vladimir.Sabelnikov@onera.fr
* ONERA/DEFA, Centre de Palaiseau, Chemin de la Hunière, 91761 Palaiseau, France
**Department of Applied Mechanics, Chalmers University of Technology, 412 96, Gothenburg, Sweden

Abstract
In order to determine the mean rate of product creation within the framework of the Turbulent Flame Closure (TFC) model of premixed combustion, the model is combined with a simple closure of turbulent scalar flux developed recently by the present authors based on the flamelet concept of turbulent burning. The model combination is assessed by numerically simulating statistically planar, one-dimensional, developing premixed flames that propagate in frozen turbulence. The mean rate of product creation yielded by the combined model decreases too slowly at the trailing edges of the studied flames, with the effect being more pronounced at longer flame-development times and larger ratios of rms turbulent velocity u' to laminar flame speed S_L. To resolve the problem, the above closure of turbulent scalar flux is modified and the combination of the modified closure and TFC model yields reasonable behaviour of the studied rate. In particular, simulations indicate an increase in the mean combustion progress variable associated with the maximum rate by flame-development time and u'/S_L, in line with available DNS data. Finally, the modified closure is validated by computing conditioned velocities and turbulent scalar fluxes in six impinging-jet flames and the use of the TFC model for simulating such flames is advocated.

Introduction
The TFC model of premixed turbulent combustion put forward by Prudnikov [1], extended by Zimont [2], and further developed and validated in Refs. [3, 4] is widely used in CFD studies of various flames. The model provides a joint closure

$$-\nabla \cdot \overline{\rho \mathbf{u}'' c''} + \overline{W} = \nabla \cdot (D_t \nabla \tilde{c}) + U_t \left| \nabla \tilde{c} \right| \tag{1}$$

of the two terms on the right hand side (RHS) of the well-known [5] balance equation

$$\frac{\partial}{\partial t} \left(\bar{\rho} \tilde{c} \right) + \nabla \cdot \left(\bar{\rho} \tilde{\mathbf{u}} \tilde{c} \right) = -\nabla \cdot \overline{\rho \mathbf{u}'' c''} + \overline{W}. \tag{2}$$

Here, t is time, $\mathbf{u}$ is the flow velocity vector, c is the combustion progress variable, ρ is the gas density, W is the mass rate of product creation, D_t and U_t are turbulent diffusivity and burning velocity, respectively, $\bar{q}$ is the Reynolds-averaged value of a quantity q with $q' \equiv q - \bar{q}$, and $\tilde{q} \equiv \overline{\rho q}/\bar{\rho}$ is the Favre-averaged value of a quantity q with $q'' \equiv q - \tilde{q}$.

The simplicity and numerical efficiency of the joint closure given by Eq. (1) makes it particularly interesting for multidimensional RANS simulations of combustion in various engines and the closure is implemented into many commercial CFD codes used for these purposes. However, the model does not yield a separate closure of the reaction term $\overline{W}$ and this limitation impedes applying the model for studying certain important issues, e.g. pollutant formation in premixed turbulent flames.

The problem can be overcome by combining the discussed joint closure with a model of the turbulent scalar flux $\overline{\rho \mathbf{u}'' c''}$ and, subsequently, by evaluating $\overline{W}$ from Eq. (1). However, because the mainstream approach to simulating the flux consists of numerically solving a complicated balance equation for $\overline{\rho \mathbf{u}'' c''}$, which involves a number of unclosed terms and tuning constants, as reviewed elsewhere [6], the combination of such an approach with the TFC model would destroy the key advantages of the latter tool, such as simplicity, numerical efficiency, and the lack of tuning parameters.

Therefore, in order to calculate the rate $\overline{W}$ from Eq. (1) and to retain the above merits of the TFC model, a simple closure of the turbulent scalar flux is required. The first attempt to propose such a simple closure was undertaken by Zimont and Biagioli [7, 8], but certain features of their model were put into question in Refs. [6, 9].

Another simple model for evaluating the normal (to the mean flame brush) component of $\overline{\rho \mathbf{u}'' c''}$ was recently developed by the present authors [9] for the flamelet regime of premixed combustion. The model was validated [9] by computing conditioned velocities and turbulent scalar fluxes measured by Cho et al. [10], Cheng and Shepherd [11], Li et al. [12], and Stevens et al. [13] in six premixed flames each stabilized in an impinging jet.

The current work was initially aimed at (i) further assessing this simple model and (ii) investigating its compatibility with the TFC model in order to evaluate the rate $\overline{W}$ from Eq. (1). However, the obtained results indicated that the former model had to be improved in order to be compatible with the TFC model. The present paper is mainly focused on the latter point, while the results of qualitatively testing the former model (improved here) are reported in an accompanying article [14].

In the next section, the problem is stated and an analytical solution is presented in the third section. The obtained results are discussed in the fourth section. The improved model is applied to the aforementioned six impinging-jet flames in the fifth section.

Statement of the Problem

Let us consider a statistically planar, one-dimensional, developing premixed flame that propagates from right to left in frozen turbulence. The flame expansion and mean structure are described by Eq. (2) and the following Favre-averaged continuity equation

$$\frac{\partial \bar{\rho}}{\partial t} + \frac{\partial}{\partial x}\left(\bar{\rho}\tilde{u}\right) = 0. \tag{3}$$

Here, x is spatial coordinate and u is the x-component of the flow velocity vector. The following analysis will be performed in the coordinate framework attached to the mean flow of the unburned mixture, i.e. $\bar{u}(-\infty) = 0$.

We assume that the probability of finding intermediate values of $0 < c < 1$ is much less than unity everywhere so that the well-known BML expressions [5, 15]

$$\rho_b \bar{c} = \bar{\rho}\tilde{c} = \frac{\tilde{c}}{1 + \tau\tilde{c}}, \tag{4}$$

$$\overline{\rho u'' c''} = \bar{\rho}\tilde{c}(1-\tilde{c})(\bar{u}_b - \bar{u}_u) = \bar{\rho}(1-\tilde{c})(\tilde{u} - \bar{u}_u) = (1-\bar{c})(\tilde{u} - \bar{u}_u) = \frac{\rho_b}{\bar{\rho}}(1-\bar{c})(\bar{u} - \bar{u}_u) \tag{5}$$

hold. Here, $\tau = \rho_u/\rho_b - 1$ is the heat-release factor, subscripts u and b designate unburned and burned mixture, respectively. For simplicity, all relevant quantities will be normalized using the density of the unburned gas in the following, i.e. symbols ρ and W will designate ρ/ρ_u and W/ρ_u, respectively, and, accordingly, $\rho_u = 1$.

The turbulent transport term on the RHS of Eq. (2) is closed invoking Eq. (5) and the following simple expression

$$(1-\bar{c})\nabla\cdot\bar{\mathbf{u}}_u = \overline{[(\mathbf{u}_u)'_f\cdot(\mathbf{n}')_f]}_f\overline{|\nabla c|} = bu'\overline{|\nabla c|} = bu'\overline{\Sigma} = \frac{bu'}{S_L}\overline{W} \tag{6}$$

obtained and validated recently by the the present authors [9]. Here, S_L is the laminar flame speed, $\overline{\Sigma} = \overline{|\nabla c|}$ is flame surface density, u' is the rms turbulent velocity at the leading edge of turbulent flame brush, $b = 1.1$ is a constant, $\mathbf{n} = -\nabla c/|\nabla c|$ is the unit vector normal to flamelet, subscript f designates surface-averaged quantities, i.e. $\bar{q}_f \equiv \overline{q|\nabla c|}/\overline{|\nabla c|}$, and $(q)'_f \equiv q - (\bar{q})_f$. Equation (6) allows for $\overline{W} = S_L\overline{\Sigma}$ in the flamelet regime of premixed combustion and invokes the following assumption $\overline{[(\mathbf{u}_u)'_f\cdot(\mathbf{n}')_f]}_f = bu'$.

Within the framework of the TFC model, Eqs. (1)-(4) have exact solution

$$\bar{c} \;=\; 1 \;-\; \frac{1}{2}\,\mathrm{erfc}\left(\xi\sqrt{\pi}\right) \;=\; 1 \;-\; \sqrt{\frac{1}{\pi}}\int_{\xi\sqrt{\pi}}^{\infty}\mathrm{e}^{-\zeta^2}d\zeta, \tag{7}$$

as proved elsewhere [16]. Here,

$$\xi = \frac{x - x_f(t)}{\Delta_t(t)}, \tag{8}$$

$$x_f = x_f(t=0) - \int_0^t U_t(\vartheta)d\vartheta \tag{9}$$

is the spatial coordinate of an iso-surface characterized by $\bar{c} = 0.5$, and

$$\Delta_t = \left(4\pi\int_0^t D_t(\vartheta)d\vartheta\right)^{1/2} \tag{10}$$

is the mean flame brush thickness determined using the maximum gradient method.

A particular goal of the present study is to investigate the behavior of the rate $\overline{W}$ calculated using Eqs. (2)-(10).

Solution

Substitution of a $\tilde{c}(\xi)$ into Eq. (3), followed by integration from $-\infty$ to ξ yields

$$\tilde{v} = \frac{1}{\bar{\rho}} - 1 + \Gamma\frac{1}{\bar{\rho}}\int_{-\infty}^{\xi}\zeta\frac{d\bar{\rho}}{d\zeta}d\zeta, \tag{11}$$

where $v \equiv u/U_t$ is the normalized velocity and

$$\Gamma \equiv \frac{1}{U_t}\frac{d\Delta_t}{dt}. \tag{12}$$

To find a solution for the velocity $\bar{u}_u$ conditioned on unburned mixture, let us rewrite Eq. (2) in the following form [17]

$$\frac{\partial}{\partial x}[(1-\bar{c})\bar{u}_u] = \frac{\partial\bar{c}}{\partial t} - \overline{W} \tag{13}$$

using Eqs. (3), (4), and (5). Substitution of a $\bar{c}(\xi)$ and Eq. (6) into Eq. (13) yields

$$\frac{\partial\bar{v}_u}{\partial\xi} = \frac{1}{1+s_L}\frac{d\bar{c}}{d\xi}\frac{\bar{v}_u + 1 - \Gamma\xi}{1-\bar{c}}, \tag{14}$$

where $s_L = S_L/(bu')$ is the normalized laminar flame speed. One can easily check by substitution that Eq. (14) supplemented with the boundary condition of $\bar{v}_u(-\infty) = \bar{v}(-\infty) = 0$ has the following analytical solution

$$\bar{v}_u = (1-\bar{c})^{-s} - 1 - \Gamma s(1-\bar{c})^{-s} \int_{-\infty}^{\xi} (1-\bar{c})^{s-1} \zeta \frac{d\bar{c}}{d\zeta} d\zeta, \tag{15}$$

where $s \equiv (1+s_L)^{-1} < 1$. Note that $\bar{v}_u \to \infty$ as $\bar{c} \to 1$.

Equations (6) and (15) result in the following expression

$$\omega \equiv \frac{\Delta_t \overline{W}}{U_t} = (1-s) \left[(1-\bar{c})^{-s} - \Gamma \left(\xi + s(1-\bar{c})^{-s} \int_{-\infty}^{\xi} (1-\bar{c})^{s-1} \zeta \frac{d\bar{c}}{d\zeta} d\zeta \right) \right] \frac{d\bar{c}}{d\xi} \tag{16}$$

for evaluating the normalized mean rate ω of product creation. It is worth noting that, for the profile of $\bar{c}(\xi)$ invoked in the present simulations, ω tends slowly to zero at the trailing edge of flame brush. For instance, at the trailing edge of a hypothetical fully-developed flame, $\xi \to \infty$, $\Gamma = 0$, and Eq. (16) yields

$$\omega \to (1-s)(2\pi\xi)^s \mathrm{e}^{(s-1)\pi\xi^2} \tag{17}$$

using Eq. (7). If a ratio of S_L/u' is low, then the parameter s is slightly smaller than unity and a decrease in ω with ξ is weakly pronounced, as shown in Fig. 1.

The above solution involves the normalized ratio Γ defined by Eq. (12). During an early stage of flame development, turbulent burning velocity is significantly less than its fully-developed value $U_{t,\infty}$ and Γ is large. As the flame develops, Γ decreases due to an increase in U_t, which tends to $U_{t,\infty}$, and a decrease in the rate of the growth of the mean flame brush thickness. In a hypothetical fully-developed flame, $\Gamma = 0$. The highest value of Γ is associated with a laminar flame embedded in a turbulent flow at $t = 0$. In such a case, Γ scales as u'/S_L at $t \to 0$, because $U_t \to S_L$ and $d\Delta_t/dt \propto u'$ according to the Taylor theory of turbulent diffusion [18].

Results reported here were obtained invoking the following expressions

$$\Delta_t^2 = 4\pi L^2 \theta \left[1 - \theta^{-1} \left(1 - \mathrm{e}^{-\theta} \right) \right], \tag{18}$$

$$U_t = S_L + C_U u' Da^{1/4} \left[1 + \theta^{-1} \left(\mathrm{e}^{-\theta} - 1 \right) \right]^{1/2}, \tag{19}$$

where L and $\tau_t = L/u'$ are the integral turbulent length and time scales, respectively, $\theta = t/\tau_t$ is the normalized time, $Da = \tau_t/\tau_c$ is the Damköhler number, $\tau_c = a_u/S_L^2$ is the chemical time scale, a_u is the molecular heat diffusivity of the unburned mixture, and $C_U = 0.4$ is a constant. Equation (18) may be obtained by substituting $D_t = u'L(1-\mathrm{e}^{-\theta})$, which results from the Taylor theory of turbulent diffusion [18], into Eq. (10) and is supported by experimental data reviewed elsewhere [1, 4]. Equation (19) is based on Eq. (18), as discussed elsewhere [4]. The domain of applicability of Eqs. (18)-(19) is bounded, e.g. Eq. (18) does not hold at $\theta \gg 1$ and, probably, at $u' \ll S_L$.

Results and Discussion

Here, we restrict ourselves solely to analyzing the behaviour of the rate ω, while the simulated profiles of the normalized scalar flux $\overline{\rho v'' c''}$ are reported in [14].

Dotted-dashed lines (curves 1) in Fig. 1 indicate that a decrease in the mean rate of product creation, calculated using Eq. (16), is too slow at the trailing edge of flame brush

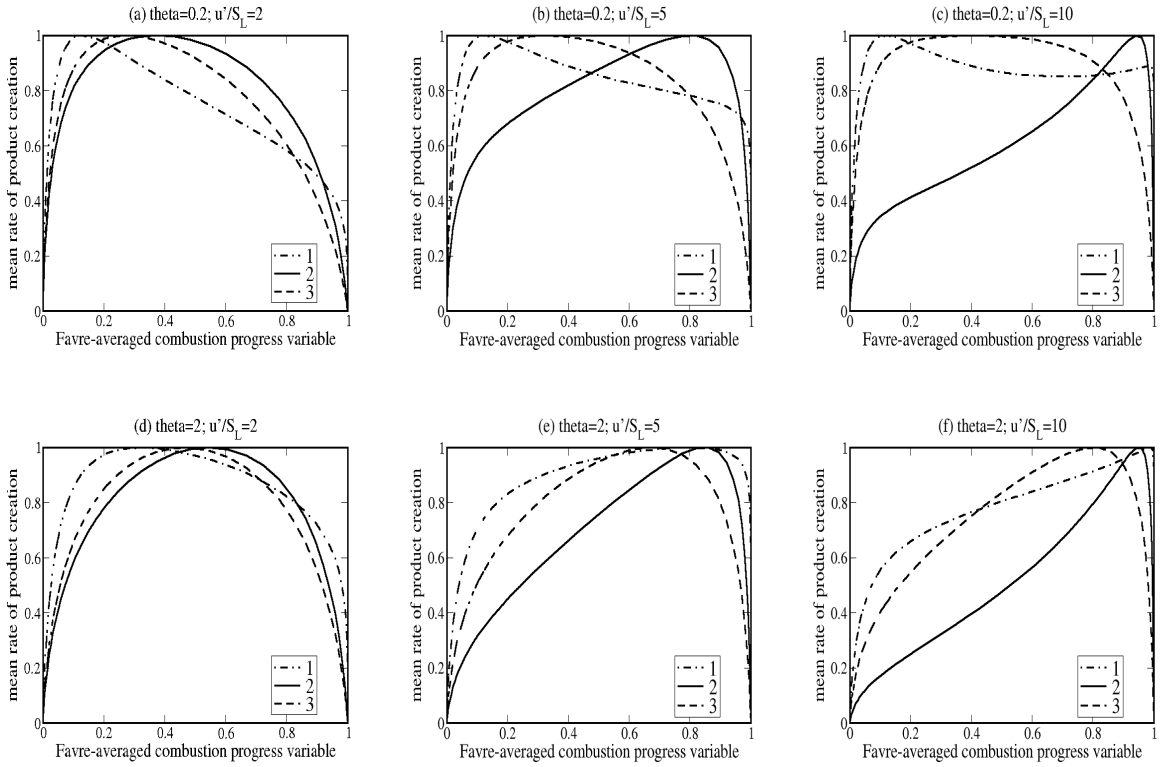

Figure 1: Dependencies of the normalized mean rate of product creation $\omega/\max\{\omega(\xi)\}$ on the Favre-averaged combustion progress variable $\tilde{c}$, calculated at various normalized flame development times θ and various ratios of u'/S_L, specified in headings. Curves 1, 2, and 3 have been obtained using $b = 1.1$, Eq. (20) with $b_1 = 1.7$ and $q = 0.5$, and Eq. (23) with $b_2 = 2.43$ and $q = p = 0.5$, respectively.

and ω is finite even if $1 - \bar{c} \ll 1$. In line with Eq. (17), the effect is strongly increased by u'/S_L (cf. curves 1 in Figs. 1a and 1c or Figs. 1d and 1f). Moreover, the effect is more pronounced at longer flame-development times (cf. curves 1 in Figs. 1a and 1d or Figs. 1c and 1f). As a result, the integral $\int_{-\infty}^{\xi(\tilde{c})} \omega d\zeta$ may be substantially lower than unity even if $1 - \tilde{c} \ll 1$, but u'/S_L is sufficiently large, see Fig. 2a. Therefore, the use of Eq. (6) in order to evaluate the rate $\overline{W}$ from Eq. (1) in multidimensional simulations may result in substantially underestimating the total burning rate, with the effect being increased by θ (cf. thin and bold lines in Fig. 2a) and especially by u'/S_L (cf. dotted-dashed, solid, and dashed lines therein). Furthermore, due to a strong increase in $\bar{v}_u$ and a slow decrease in ω as $\tilde{c} \to 1$, the two terms on the RHS of Eq. (2) may be finite and balance one another even if $1 - \tilde{c} \ll 1$, see curves 3 and 4 in Fig. 3a. All these trends indicate that Eq. (6) with a constant b is incompatible with the TFC model.

To resolve the problem and to obtain a stronger decrease in the normalized rate ω as $\tilde{c} \to 1$, the constant b in Eq. (6) may be replaced with a decreasing function $b(\tilde{c})$, which vanishes as $\tilde{c} \to 1$, in line with the DNS data by Im et al. [17] (see dotted-dashed line in Fig. 6 in the cited paper). If, for instance,

$$b = b_1(1 - \bar{c})^q, \tag{20}$$

where $0 < q < 1$, then, Eqs. (2)-(10) yield

$$\frac{\partial \bar{v}_u}{\partial \xi} = \frac{d\bar{c}}{d\xi} \frac{\bar{v}_u + 1 - \Gamma\xi}{1 - \bar{c} + s_{L1}(1 - \bar{c})^{1-q}} \tag{21}$$

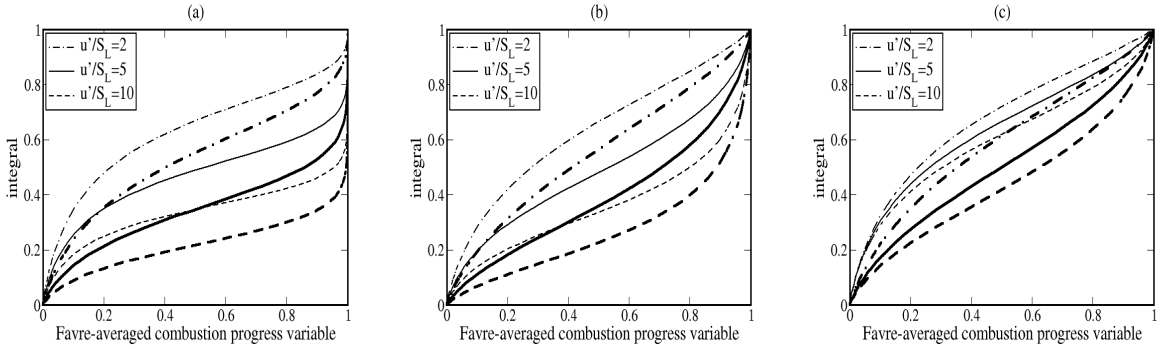

Figure 2: Dependencies of the integral $\int_{\infty}^{\xi(\tilde{c})} \omega d\zeta$ on $\tilde{c}$ associated with the up integration limit, calculated at different u'/S_L specified in legends. Thin and thick lines have been obtained for $\theta = 0.2$ and 2, respectively. (a) $b = 1.1$, (b) Eq. (20) with $b_1 = 1.7$ and $q = 0.5$, and (c) Eq. (23) with $b_2 = 2.43$ and $q = p = 0.5$.

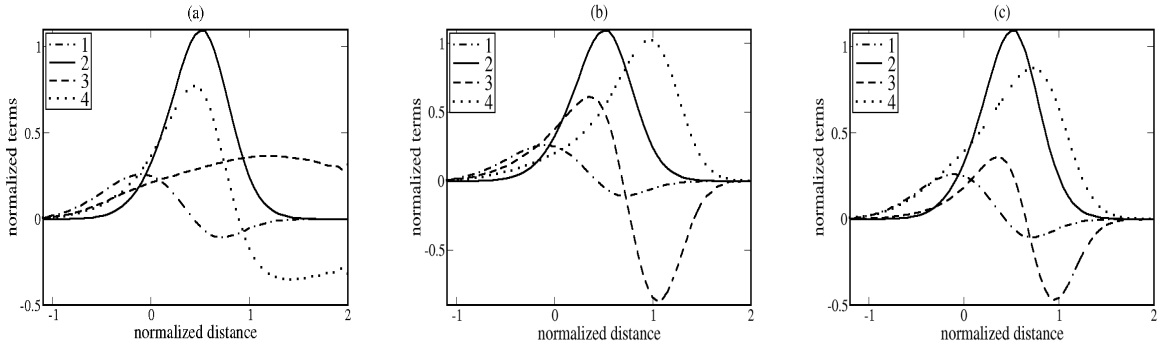

Figure 3: Dependencies of various normalized terms on the normalized distance ξ, computed at $\theta = 2$ and $u'/S_L = 10$ using either (a) $b = 1.1$, or (b) Eq. (20) with $b_1 = 1.7$ and $q = 0.5$, or (c) Eq. (23) with $b_2 = 2.43$ and $q = p = 0.5$. 1 - $(\Delta_t/U_t)\bar{\rho}\partial\tilde{c}/\partial t$, 2 - $\bar{\rho}\tilde{v}\mathrm{d}\tilde{c}/\mathrm{d}\xi$, 3 - $-\partial\overline{\rho v'' c''}/\partial\xi$, 4 - ω. $S_L = 0.4$ m/s, $a_u = 0.222$ cm^2/s, $\tau = 6$, $L = 5$ mm.

and

$$\omega \equiv \frac{\Delta_t \overline{\Omega}}{U_t} = \frac{\bar{v}_u + 1 - \Gamma\xi}{1 + s_{L1}(1-\bar{c})^q} \frac{d\bar{c}}{d\xi}, \tag{22}$$

where $s_{L1} = S_L/(b_1 u')$. The former equation was numerically integrated using the method of Runge-Kutta, followed by evaluation of the normalized rate using Eq. (22).

Results obtained with $q = 0.5$ and $b_1 = 1.7$ (the choice of this value of b_1 will be explained in the next section) are shown in solid lines (curves 2) in Fig. 1, as well as in Figs. 2b and 3b. This modification of the model substantially improves the behaviour of the rate ω at the trailing edge of the flame brush (cf. solid and dotted-dashed lines in Fig. 1, or Figs. 2a and 2b, or Figs. 3a and 3b), but the improvement is insufficient at high ratios of u'/S_L (see solid lines in Figs. 1c and 1e, or dashed lines in Fig. 2b).

To further improve the model, it is worth remembering that Eq. (6) was obtained by assuming that $[\overline{(\mathbf{u}_u)'_f \cdot (\mathbf{n}')_f}]_f = bu'$ [9]. In the limit case of $u'/S_L \to \infty$, the influence of flamelets on turbulence appears to be negligible and the above correlation seems to vanish. Therefore, it is tempting to assume that b in Eq. (6) decreases when u'/S_L increases, e.g. $b \propto (1 + u'/S_L)^{-p}$, where $p > 0$. Combining this assumption with Eq. (20), we have

$$b = b_2 \frac{(1-\bar{c})^q}{(1+u'/S_L)^p} \tag{23}$$

and Eqs. (21)-(22) hold provided that s_{L1} is replaced with $s_{L2} = S_L/(b_2 u')$.

Results obtained with $q = p = 0.5$ and $b_2 = 2.43$ (the choice of this value of b_2 will be explained in the next section) are shown in dashed lines (curves 3) in Fig. 1, as well as in Figs. 2c and 3c. The use of Eq. (23) substantially improves the behaviour of the rate ω at the trailing edge of the flame brush even at ratios of u'/S_L as large as 10. Because the flamelet concept used to obtain Eq. (6) in Ref. [9] is not valid in highly turbulent flames, as reviewed elsewhere [6], testing the above model at ratios of u'/S_L significantly larger than 10 does not seem to be meaningful. It is also worth noting that although Eq. (22) allows ω to be negative if $\xi > 0$ and Γ is sufficiently large, we did not observe negative ω in our simulations when Eq. (23) with $q = p = 0.5$ and $b_2 = 2.43$ was used.

As a whole, dashed lines in Fig. 1 appear to indicate reasonable behaviour of the rate ω, which seems to be consistent with available data. Even if quantitatively testing our numerical results shown in Fig. 1 does not seem to be possible for a number of reasons (e.g. the shortage of available experimental data, the strong dependence of the computed $\omega(\tilde{c})$-curves on flame-development time and the ratio of u'/S_L, the lack of target-directed investigation of the influence of either θ or u'/S_L on the shape of the $\omega(\tilde{c})$-curve, etc.), qualitative assessment could be done by invoking DNS data on flame surface density $\overline{\Sigma}$ and mean scalar dissipation rate $\bar{\chi}_c$, because the mean rate $\overline{W}$ is commonly considered to be proportional to both $\overline{\Sigma}$ and $\bar{\chi}_c$ in the flamelet regime of premixed turbulent combustion.

In particular, our simulations yield an increase in the value $\tilde{c}_m$, associated with the maximum of $\omega(\tilde{c})$, by u'/S_L (cf. Figs. 1a, 1b, and 1c or Figs. 1d, 1e, and 1f) and by flame-development time (cf. Figs. 1a and 1d, or Figs. 1b and 1e, or Figs. 1c and 1f) and the same trends were already documented in DNS.

First, Hult et al. [19] claimed that their DNS indicated a shift of the observed peak in $\overline{\Sigma}(\bar{c})$ "towards the burned side with increasing u'/S_L" (see Fig. 3 in the cited paper). This trend is also pronounced in Fig. 2 by Chakraborty et al. [20], Fig. 7 by Han and Huh [21], and Fig. 7 by Lee and Huh [22].

Second, DNS by Swaminathan and Grout [23] indicated a shift of the observed peak in $\bar{\chi}_c(\tilde{c})$ towards the trailing edge of flame brush, as the flame developed, and a similar shift was observed for $\overline{\Sigma}(\bar{c})$ in a couple of DNS studies, see Fig. 8b by Trouvé and Poinsot [24], Fig. 3 by Hult et al. [19], Fig. 2 by Chakraborty et al. [20], Fig. 7 by Han and Huh [21], and Fig. 7 by Lee and Huh [22].

The fact that the same trends in the dependence of $\tilde{c}_m$ on u'/S_L and flame-development time were observed in our simulations and previous DNSs qualitatively support the present model. Other results that qualitatively support it are discussed elsewhere [14].

A Quantitative Test

As shown above, substitution of Eq. (23) into Eq. (6) allows us to obtain reasonable profiles of $\overline{W}$ in developing statistically planar, one-dimensional premixed turbulent flames, whereas Eq. (6) with $b = 1.1$ yields too slow decrease in $\overline{W}$ as $\tilde{c} \to 1$. However, the latter closure was quantitatively validated by simulating six impinging-jet flames [9], while the capability of the modified closure for predicting the same experimental data is unclear. Accordingly, the same six flames were numerically studied not only setting $b = 1.1$, but also invoking Eq. (23). Because the sole difference between the present computations and simulations discussed in detail in Ref. [9] consists of the use of Eq. (23) instead of $b = 1.1$,

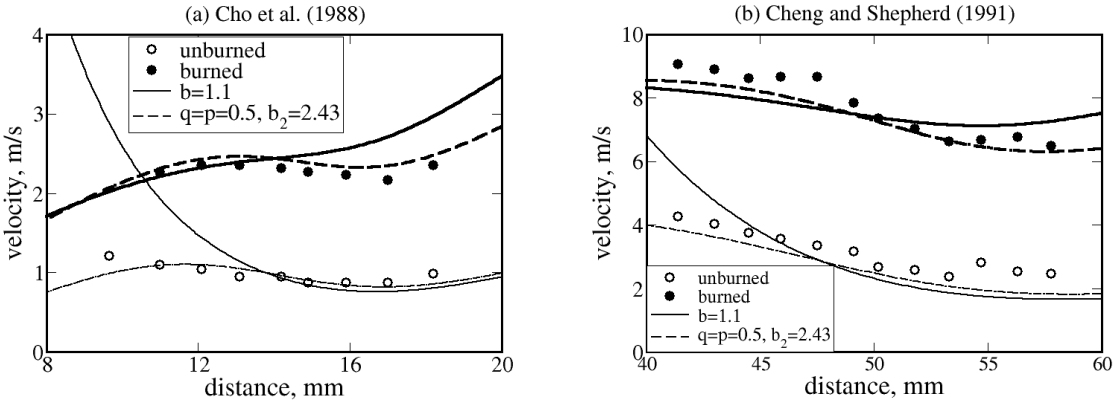

Figure 4: Conditioned axial velocities (a) in case 1 studied by Cho et al. [10] and (b) in flame s9 investigated by Cheng and Shepherd [11]. Symbols show experimental data. Curves were computed using Eq. (6) either with $b = 1.1$ or invoking Eq. (23) with $q = p = 0.5$ and $b_2 = 2.43$. Thin and bold lines show velocities conditioned to unburned and burned mixtures, respectively.

we refer the interested reader to Ref. [9] and restrict ourselves to reporting results.

Figures 4 and 5 show that the new closure given by Eq. (23) yields approximately the same agreement with the experimental data obtained by Li et al. [12] from flame h4 (the conditions of the measurements are reported in Table 1) and improves agreement with the experimental data obtained from the other five flames.

It is worth stressing that we restricted ourselves to coarsely tuning the power exponents q and p. At first, we simulated the six flames invoking Eq. (20) with $q = 0$, 0.2, and 0.5 and tuned the constant b_1 for each q by varying b_1 with step 0.1. The tuned values of b_1 are equal to 1.1 for $q = 0$ (the original model [9]), 1.3 for $q = 0.2$, and 1.7 for $q = 0.5$, with the best agreement with the experimental data being obtained for $q = 0.5$. Then, we calculated $b_{2,k} = 1.7/(1 + u'_k/S_{L.k})^p$ for every flame ($k = 1, \ldots, 6$) and $p = 0.5$ or 1, followed by evaluation of the mean values $b_2(p) = \sum_{k=1}^{6} b_{2,k}(p)/6$. Because agreement with the experimental data was better for $p = 0.5$ and $b_2(p = 0.5) = 2.43$, this set of the model parameters was finally selected when computing results shown in Figs. 4 and 5. Thus, we have run simulations with five sets of model parameters, i.e. (i) $q = p = 0$ and $b = 1.1$, (ii) $q = 0.2$, $p = 0$, and $b = 1.3$, (iii) $q = 0.5$, $p = 0$, and $b = 1.7$, (iv) $q = p = 0.5$ and $b = 2.43$, and (v) $q = 0.5$, $p = 1$, and $b = 3.5$. The best agreement with

Table 1: Experimental conditions[a]

Flame No.	d (m)	U (m/s)	Fuel	Φ	S_L (m/s)	τ	u' (m/s)	Reference
1	0.075	5	CH_4	1.0	0.365	6.513	0.4	Cho et al. [10], case 1
2	0.1	5	C_2H_6	1.0	0.76	7.004	0.6	Cheng and Shepherd [11], s9
3	0.03	3.6	CH_4	0.89	0.307	6.077	0.25	Li et al. [12], h4
4	0.03	3.6	CH_4	0.89	0.307	6.077	0.34	Li et al. [12], h6
5	0.035	3	CH_4	1.0	0.365	6.513	0.4	Stevens et al. [13], set 2
6	0.035	2.25	CH_4	1.3	0.213	6.112	0.3	Stevens et al. [13], set 3

[a]Here, d is the distance between the jet exit and the wall, U is the mean axial flow velocity in the jet exit, and Φ is the equivalence ratio.

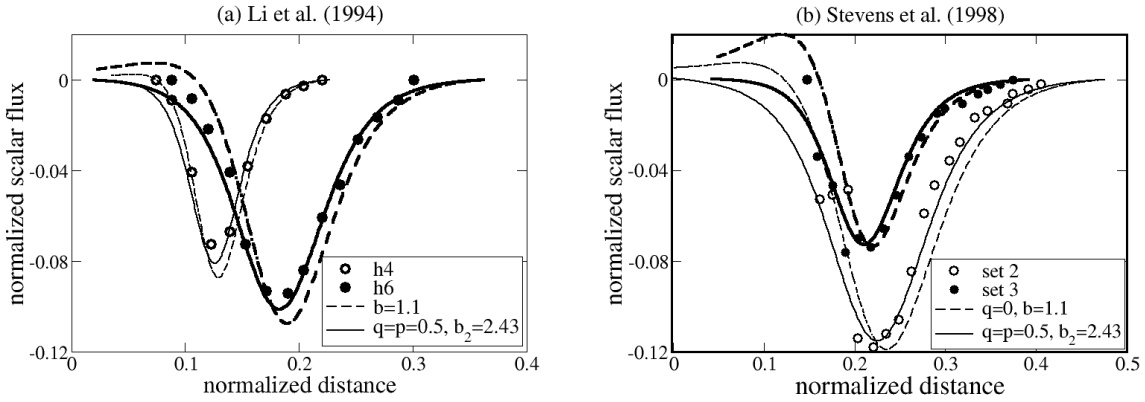

Figure 5: Normalized axial scalar flux $\overline{\rho u'' c''}/(\bar{\rho} U)$ vs. normalized distance x/d (a) in flames h4 (thin lines) and h6 (bold lines) studied by Li et al. [12] and (b) in flames "set 2" (thin lines) and "set 3" (bold lines) investigated by Stevens et al. [13]. Symbols show experimental data. Curves were computed using Eq. (6) either with $b = 1.1$ or invoking Eq. (23) with $q = p = 0.5$ and $b_2 = 2.43$.

the experimental data was observed in cases (iii) and (iv). Because the numerical results obtained in the two best cases were very close to another, only data computed in case (iv) are plotted in Figs. 4 and 5. More experimental or DNS data are required to tune q and p more precisely.

Note that the use of the TFC model for simulating impinging-jet flames may be put into question by referring to a paper by Bray et al. [25] who claimed that the model failed in predicting the burning rate in flames s9, h4, and h6 (i.e flames Nos. 2-4 in Table 1). More specifically, Bray et al. [25] have found that the following simple expression

$$\overline{W} = U_t \, |\nabla \tilde{c}| \tag{24}$$

yields wrong dependence of $\overline{W}$ on $\tilde{c}$ if the turbulent burning velocity U_t is evaluated using local Favre-averaged turbulence characteristics, which depend substantially on $\tilde{c}$ and are strongly affected by unburned-burned intermittency.

As pointed out elsewhere [26], the model tested by Bray et al. [25] differs substantially from the TFC model. In particular, the latter model does not address $\overline{W}$, but provides the joint closure given by Eq. (1), and this difference between Eq. (24) and the TFC model is substantial. Indeed, let us consider Eqs. (2) and (3) closed invoking Eq. (1). Along the axis of an impinging-jet flame, they read [25, 27]

$$\frac{d\bar{\varrho}\tilde{w}}{dz} + 2\bar{\varrho}\tilde{g} = 0, \tag{25}$$

$$\underbrace{\bar{\rho}\tilde{w}\frac{d\tilde{c}}{dz}}_{I} = \underbrace{-\frac{d}{dz}\overline{\rho w'' c''}}_{II} + \underbrace{\Omega}_{III} + \underbrace{2\bar{\rho}\tilde{c}(1-\tilde{c})(\bar{g}_b - \bar{g}_u)}_{VI} = \underbrace{d_t \frac{d}{dz}\left(\bar{\varrho}\frac{d\tilde{c}}{dz}\right)}_{IV} - \underbrace{u_t \frac{d\tilde{c}}{dz}}_{V}, \tag{26}$$

with term VI being commonly neglected [8, 9, 25]. Here, $z = x/d$, $w = u/U$, $g = (d/U)(\partial v/\partial r)_{r=0}$, $\Omega = \overline{W} d/U$, $u_t = U_t/U$, and $d_t = D_t/(Ud)$ are the normalized axial distance, axial velocity, radial gradient of the radial velocity, mean mass rate of product creation, burning velocity, and turbulent diffusivity, respectively. The results of the aforementioned numerical simulations of the six impinging-jet flames, performed by neglecting

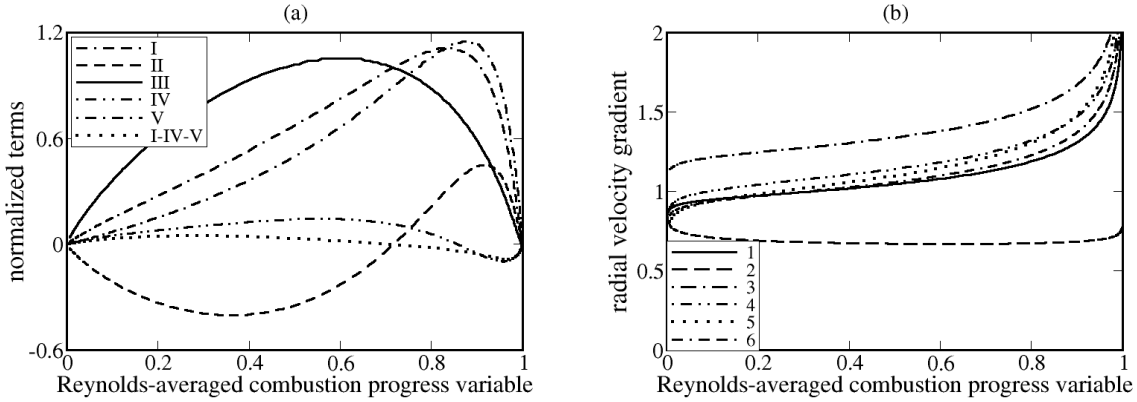

Figure 6: (a) Different terms in Eq.(26), normalized using ρ_u, d, and U, vs. the Reynolds-averaged combustion progress variable. Curves have been computed for the flame h6 investigated by Li et al. [12]. Term numbers are specified in legends. (b) The radial gradient of the Favre-averaged radial velocity, normalized using d and U, vs. the Reynolds-averaged combustion progress variable. Flame numbers are specified in legends.

term VI [9], allow us to evaluate terms I-V in Eq. (26), provided that the normalized burning velocity and diffusivity are closed. To do so, the following two expressions

$$u_t = \int_0^1 \Omega d\bar{c}, \qquad\qquad d_t = \frac{\delta_t^2}{\pi}\int_0^1 \tilde{g} d\bar{c} \tag{27}$$

were invoked, where $\delta_t = \Delta_t/d$ is the normalized flame brush thickness. The former closure results from integration of Eq. (26) with term VI being neglected. To substantiate the latter closure, let us substitute Eqs. (4) and (7) into Eq. (26). Then, we obtain

$$\bar{\rho}\tilde{w} = \frac{d_t}{\delta_t}\left(-2\pi\xi\bar{\rho} - \frac{\tau}{\tau+1}\mathrm{e}^{-\pi\xi^2}\right) - u_t. \tag{28}$$

Differentiating this equation and using Eqs. (4), (7), and (25), we arrive at

$$2\bar{\rho}\tilde{g} = -\frac{1}{\delta_t}\frac{d\bar{\rho}\tilde{w}}{d\xi} = 2\pi\bar{\rho}\frac{d_t}{\delta_t^2}. \tag{29}$$

Results computed for flame h6 investigated by Li et al. [12] are shown in Fig. 6a and similar results were obtained for the other five flames. The transport terms II and IV have opposite signs, with the magnitude of the former term being comparable with the magnitudes of terms I, III, and V. Therefore, the source terms III and V depend differently on the mean combustion progress variable and Eq. (24) disputed by Bray et al. [25] is inconsistent with the TFC model.

We may note also that the difference in terms I, IV, and V (see dotted line) is significantly less than terms I and V, thus indicating that Eq. (1) holds in the studied flames. Furthermore, Eq. (29) shows that the normalized radial gradient $\tilde{g}$ does not depend on $\bar{c}$ within the framework of the TFC model, provided that Eq. (7) well approximates the axial profile of $\bar{c}(\xi)$. Our simulations (see Fig. 6b) do show that $\tilde{g}$ (computed as discussed in Ref. [9]) is approximately constant in the largest part of a flame brush, with the exception of the trailing edge ($\bar{c} > 0.8$), in all the six studied cases.

Conclusions

In order to determine the mean rate $\overline{W}$ of product creation within the framework of the TFC model of premixed combustion, the model was proposed to be combined with a simple closure of turbulent scalar flux, see Eq. (6), developed recently by the present authors [9] based on the flamelet concept of turbulent burning.

The model combination was assessed by simulating statistically planar, one-dimensional, developing premixed flames that propagated in frozen turbulence. Because the computed mean rate of product creation decreases too slowly as $\tilde{c} \to 1$, especially at large u'/S_L, the closure given by Eq. (6) with a constant b is incompatible with the TFC model.

To resolve the problem, the closure was modified, i.e. the constant b in Eq. (6) was replaced with a function $b(\bar{c}, u'/S_L)$, given by Eq. (23).

The combination of the modified closure and the TFC model yields reasonable behaviour of the rate $\overline{W}$. In particular, the present simulations indicate an increase in the mean combustion progress variable associated with the maximum of $\overline{W}$ as a function of $\bar{c}$ by flame-development time and u'/S_L, in line with available DNS data.

The modified closure was validated by computing conditioned velocities and turbulent scalar fluxes in six different impinging-jet flames.

Acknowledgments

The first author (VS) was supported by ONERA. The second author (AL) was supported by the Swedish Energy Agency and by the Chalmers Combustion Engine Research Center.

References

[1] Prudnikov, A.G., "Burning of homogeneous fuel-air mixtures in a turbulent flow", in *Physical Principles of the Working Process in Combustion Chambers of Jet Engines*, Ed. by Raushenbakh, B.V., Springfield: Clearing House for Federal Scientific & Technical Information, pp. 244-336, 1967.

[2] Zimont, V.L., "Theory of turbulent combustion of a homogeneous fuel mixture at high Reynolds number", *Combust. Explos. Shock Waves* 15: 305-311 (1979).

[3] Zimont, V.L., Lipatnikov, A.N., "A numerical model of premixed turbulent combustion", *Chem. Phys. Reports* 14: 993-1025 (1995).

[4] Lipatnikov, A.N., Chomiak, J., "Turbulent flame speed and thickness: phenomenology, evaluation, and application in multi-dimensional simulations", *Prog. Energy Combust. Sci.* 28: 1-74 (2002).

[5] Bray, K.N.C, Moss, J.B., "A unified statistical model for the premixed turbulent flame", *Acta Astronautica* 4: 291-319 (1977).

[6] Lipatnikov, A.N., Chomiak, J. "Effects of premixed flames on turbulence and turbulent scalar transport", *Prog. Energy Combust. Sci.* 36: 1-102 (2010).

[7] Zimont, V.L., Biagioli, F., "Gradient, counter-gradient transport and their transition in turbulent premixed flames", *Combust. Theory Modell.* 6: 79-101 (2002).

[8] Biagioli, F. and Zimont, V.L., "Gasdynamics modelling of counter-gradient transport in open and impinging turbulent premixed flames", *Proc. Combust. Inst.* 29: 2087-2095 (2002).

[9] Sabel'nikov, V.A., Lipatnikov, A.N. "A simple model for evaluating conditioned velocities in premixed turbulent flames", *Combust. Sci. and Tech.* 183: 588-613 (2011).

[10] Cho, P., Law, C.K., Cheng, R.K., Shepherd, I.G., "Velocity and scalar fields of turbulent premixed flames in stagnation flow", *Proc. Combust. Inst.* 22: 739-745 (1988).

[11] Cheng, R.K., Shepherd, I.G., "The influence of burner geometry on premixed turbulent flame propagation", *Combust. Flame* 85: 7-26 (1991).

[12] Li, S.C., Libby, P.A., Williams, F.A., "Experimental investigation of a premixed flame in an impinging turbulent stream", *Proc. Combust. Inst.* 25: 1207-1214 (1994).

[13] Stevens, E.J., Bray, K.N.C., Lecordier, B., "Velocity and scalar statistics for premixed turbulent stagnation flames using PIV", *Proc. Combust. Inst.* 27: 949-955 (1998).

[14] Lipatnikov, A.N., Sabel'nikov, V.A., "Transition from countergradient to gradient turbulent scalar transport in developing premixed turbulent flames", submitted to MCS7, 2011.

[15] Libby, P.A., Bray, K.N.C., "Countergradient diffusion in premixed turbulent flames", *AIAA J.* 19: 205-213 (1981).

[16] Lipatnikov, A.N., Chomiak, J., "Self-similarly developing, premixed, turbulent flames: a theoretical study", *Phys. Fluids* 17: 065105 (2005).

[17] Im, Y.H., Huh, K.Y., Nishiki, S., Hasegawa, T., "Zone conditional assessment of flame-generated turbulence with DNS database of a turbulent premixed flame", *Combust. Flame* 137: 478-488 (2004).

[18] Taylor, G.I., "Statistical theory of turbulence. IV. Diffusion in a turbulent air stream", *Proc. R. Soc. London* A151: 465-478 (1935).

[19] Hult, J., Gashi, S., Chakraborty, N., Klein, M., Jenkins, K.W., Cant, R.S., Kaminski, C.F., "Measurement of flame surface density for turbulent premixed flames using PLIF and DNS", *Proc. Combust. Inst.* 31: 1319-1326 (2007).

[20] Chakraborty, N., Rogerson, J.W., Swaminathan, N., "A priori assessment of closures for scalar dissipation rate transport in turbulent premixed flames using direct numerical simulation", *Phys. Fluids* 20: 045106 (2008).

[21] Han, I., Huh, K.Y., "Effects of the Karlovitz number on the evolution of the flame surface density in turbulent premixed flames", *Proc. Combust. Inst.* 32: 1419-1425 (2009).

[22] Lee, E., Huh, K.Y., "Statistically steady incompressible DNS to validate a new correlation for turbulent burning velocity in turbulent premixed combustion", *Flow, Turb. Combust.* 84: 339-356 (2010).

[23] Swaminathan, N., Grout, R.W., "Interaction of turbulence and scalar fields in premixed flames", *Phys. Fluids* 18: 045102 (2006).

[24] Trouvé, A., Poinsot, T., "Evolution equation for flame surface density in turbulent premixed combustion", *J. Fluid Mech.* 278: 1-31 (1994).

[25] Bray, K.N.C., Champion, M., Libby, P.A., "Premixed flames in stagnating turbulence part V - evaluation of models for the chemical source term", *Combust. Flame* 127: 2023-2040 (2001).

[26] Lipatnikov, A.N., "Comments on the paper "Premixed Flames in Stagnating Turbulence Part V – Evaluation of Models for the Chemical Source Term" by Bray, K.N.C., Champion, M., and Libby, P.A.", *Combust. Flame* 131: 219-221 (2002).

[27] Lipatnikov, A.N., "A test of conditioned balance equation approach", *Proc. Combust. Inst.* 33: 1497-1504 (2011).